JOURNAL OF Materials CHEMISTRY

Crystal structure and electrical properties of $K_2P_4W_{12}O_{44}$, the $m=6$ member of the series of low-dimensional conductors $K_x(PO_2)_4(WO_3)_{2m}$

Pascal Roussel,*[a] Sylvie Drouard,[b] Daniel Groult,[a] Philippe Labbé,[a] Jean Dumas[b] and Claire Schlenker[b]

[a]*Laboratoire CRISMAT, CNRS UMR 6508, ISMRA-Université de Caen, 14050 Caen Cédex, France. E-mail: p.roussel@crismat.ismra.fr*
[b]*Laboratoire d'Etudes des Propriétés Electroniques des Solides, CNRS, BP166, 38042 Grenoble Cédex 9, France*

Received 16th November 1998, Accepted 14th January 1999

A new member, $m=6$, of the series $K_x(PO_2)_4(WO_3)_{2m}$ has been isolated and studied by single crystal X-ray diffraction and electrical transport measurements. The structure corresponds to that of the MonoPhosphates Tungsten Bronzes with hexagonal tunnels (MPTBh's). It has been solved and refined to conventional $R=0.0268$ with 2342 independent reflections with $I>3\sigma(I)$. The unit cell is monoclinic (space group $P2_1/m$) with $a=6.6736(2)$, $b=5.3543(3)$, $c=11.9005(5)$ Å, $\beta=92.615(3)^\circ$. The oxygen surroundings of K, P and W atoms are described and compared with those of other members of the series including Pb-, Na- and K-based analogues. Electrical properties and correlations with structural data are discussed. Large magnetoresistance effects have been observed at low temperature and assigned to possible CDW instabilities.

1 Introduction

The phosphate tungsten bronzes form a large family of oxides with an elementary structural building principle: WO_3 slabs of octahedral ReO_3-type are interconnected by tetrahedral slices parallel to the slabs and made of PO_4 or P_2O_7 groups. This feature is generated by the fact that, in a 'perovskite cage' bounded by eight WO_6 octahedra sharing corners, a PO_4 tetrahedron can replace a WO_6 octahedron, and a P_2O_7 diphosphate group to replace two neighbouring octahedra. This causes a slight local distortion (Fig. 1) since the O–O distance in a PO_4 tetrahedron is *ca.* 2.5 Å while it is *ca.* 2.7 Å in a WO_6 octahedron.

The first publication on the subject was relative to a single crystal X-ray diffraction structural study of $Rb_xP_4W_8O_{32}$,[1] a diphosphate tungsten bronze which involves a tunnel structure (DPTBh): the tetrahedral slices contain diphosphate groups and their interconnections with WO_6 octahedra build hexagonal tunnels in which cations of large size are inserted. The members of this family exhibit monoclinic symmetry and all correspond to a series of phases with general formula $A_x(P_2O_4)_2(WO_3)_{2m}$ where m is an integer related to the thickness of the ReO_3-type slabs and A is a cation such as K^+, Ba^{2+}, Tl^+ or Rb^+. For Cs^+, the connection between corner-sharing WO_6 octahedra and P_2O_7 diphosphate groups is modified so that wide tunnels of octagonal section are formed in which Cs^+ ions can be located.[2] If the size of the inserted cation is equal to or smaller than that of K^+, the atomic arrangement changes again, and another family is obtained, the monophosphate tungsten bronzes (MPTBh). The corresponding members have the same chemical formula $A_x(PO_2)_4(WO_3)_{2m}$, but the orientation of the octahedral slabs is modified, now interconnected by PO_4 tetrahedra instead of diphosphate groups. A is a cation such as K^+, Pb^{2+}, Na^+ inserted in cages building pseudo-hexagonal tunnels; m is always an integer related to the thickness of the perovskite-type slab.

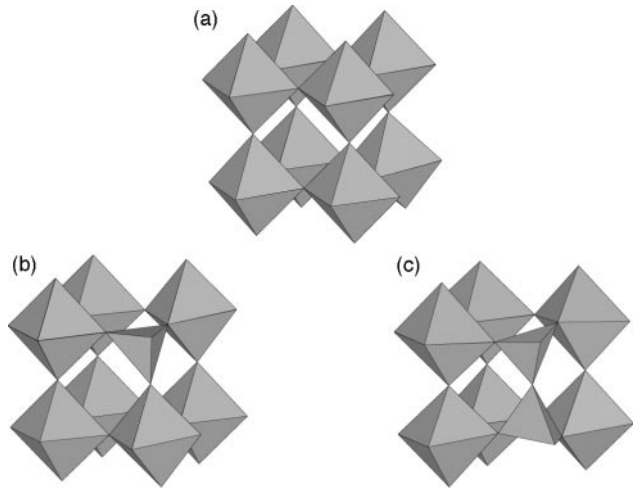

Fig. 1 Replacement of WO_6 octahedra in a structure of ReO_3-type: (a) classical perovskite cage, (b) one WO_6 octahedron is substituted for a PO_4 tetrahedron leading to monophosphate tungsten bronzes (MPTB), (c) two adjacent WO_6 octahedra sharing corners are substituted for a P_2O_7 diphosphate group leading to diphosphate tungsten bronzes (DPTB).

Recent studies have yielded interesting correlations between the electronic properties of these phosphate tungsten bronzes and crystal structure. $CsP_8W_8O_{40}$ is thus a quasi-one-dimensional (1D) conductor[3] which exhibits a localisation–delocalisation transition of the Anderson type at *ca.* 160 K.[4] On the other hand DPTBhs $KP_4W_{12}O_{44}$ and $KP_4W_{14}O_{50}$, the members $m=6$ and 7 of the series $K_x(P_2O_4)_2(WO_3)_{2m}$ respectively, have been shown to behave as quasi-two-dimensional metals down to 4 K.[5] A similar behaviour has been more recently reported for the MPTBh counterpart $K_xP_4W_8O_{32}$. In the latter a metal-to-metal transition possibly related to a charge density wave (CDW) ground state was observed at temperatures <170 K depending upon the potassium content x.[6,7] The strong correlation between the electronic and the structural properties is due to the layered structure with conducting octahedral slabs separated by insulating tetrahedral slices. This leads to quasi-two-dimensional transport properties.

Because they offer the possibility of changing both the thickness of the conducting layers through the m value and the average conduction electron density per W atom

$[(4+x)]/2m$ through the alkali metal cation content x, the series $A_x(PO_2)_4(WO_3)_{2m}$ (A = Na, K) of MPTBh compounds can be considered as providing a model system to deepen the understanding of CDW instabilities in quasi-2D conductors. However such a study requires precise information on the crystal structure, allowing calculations of the energy band structure and correlations with the electronic properties. At the present time, six compounds are known: two with $m=4$ and A = Na and K;[8,9] one with $m=6$ and A = Na[8] and three with $m=7$ and A = Na, K, Pb.[10–12] The aim of this work is to complete the study of the series and to compare the K compounds with the undoped ones which have been extensively investigated.[13] In this article, we report structural studies and electrical transport data of $KP_2W_6O_{22}$ single crystals, $m=6$ member of the series. However, for a convenient comparison of the compound with other members of the series and more particularly with the Na-based counterparts $Na_x(PO_2)_4(WO_3)_{2m}$,[8,10] the chemical formula $K_2P_4W_{12}O_{44}$ will be used.

2 Experimental

2.1 Preparation and crystal growth

Mixtures of $(NH_4)_2HPO_4$, WO_3 and K_2CO_3 in appropriate ratios were first heated in air at 600 °C for 12 h in order to decompose the phosphate and the carbonate. Because of the mixed valence of tungsten, an adequate amount of metallic powdered tungsten used as a reducing agent was added to the decomposed initial mixture before grinding. The powder was then heated in an evacuated silica ampoule at 950 °C for 48 h and slowly cooled to 25 °C.

An amount (*ca.* 2 g) of $K_xP_4W_{12}O_{44}$ polycrystalline sample was weighed and put in a quartz tube (20 cm long and 1.8 cm internal diameter), which was sealed under vacuum. After placing the tube in a horizontal furnace, a temperature gradient of *ca.* 10 °C cm^{-1} was applied along its length with the hot zone at 1200 °C and the cold zone at 1000 °C. The powder was held under these conditions for one week in order to grow single crystals by chemical transport at the cold zone. The tube was progressively cooled to 25 °C by successive steps at 1000, 800, 600, 400 and 200 °C. Dark purple crystals grew in the middle part of the tube as platelets, needles and bars with largest sizes of $6\times3\times1$ mm.

Elemental analysis for K, P and W was performed by energy dispersive X-ray spectrometry (EDS) using a Philips FEG-XL 30 scanning electron microscope.

2.2 Crystal structure determination

Films obtained with a Weissenberg camera show well defined sharp spots, no apparent diffusion and no presence of twinning, which is rather rare for samples of this family. The apparent monoclinic symmetry with ***b*** as the unique axis ($b=5.3$ Å) and a β angle near 92.6° was confirmed later by diffractometric techniques using a CAD4 Enraf-Nonius goniometer by comparison of the intensity of equivalent reflections. The values of the lattice parameters were found to be consistent with those of other potassium compounds and also of the sodium counterpart $Na_xP_4W_{12}O_{44}$. However, the ***c*** value for the title compound (11.901 Å) was found to be about half of the ***c*** parameter of the Na compound (23.78 Å) though both correspond to the same $m=6$ value. This point has been carefully verified. The only systematic absent reflections are for $0k0$ with $k=2n+1$, which is consistent with the $P2_1/m$ space group. The characteristics of the selected sample, of the collected data and of the structure refinement are given in Table 1.

Data reduction of two symmetrically equivalent spaces was performed with the XCAD4 program,[14] and corrected for scale variation based upon standards and Lorentz-polarization effects. SIR97[15] was used to find the solution, refined by full-matrix least squares with JANA98.[16] The W, P and K atoms were refined anisotropically and O atoms isotropically. The least-squares refinement [based on 2342 observed reflections with $I>3\sigma(I)$ and 58 variable parameters] converged to $R=0.0268$ and $Rw=0.0324$ with an occupancy of 50.6(3)% of the K sites, the content of the cell thus being $K_{1.012}P_2W_6O_{22}$ in good agreement with EDS analysis [$x=1.01(5)$]. Final atomic coordinates and atomic displacement parameters are listed in Table 2. Selected interatomic distances are given in Table 3.

Table 1 Structure determination parameters

Temperature/K	293
Chemical formula	$K_{1.012(2)}P_2W_6O_{22}$
M	1556.6
Space group	$P2_1/m$ (No. 11)
a/Å	6.6736(2)
b/Å	5.3543(3)
c/Å	11.9005(5)
β/°	92.615(3)
V/Å^3 ($Z=1$)	424.79(4)
D_c/g cm^{-3}	6.084
Crystal form	Platelet delimited by (100) (010) and (001)
Crystal size/μm	$160\times70\times8$
Crystal color	Dark purple
Diffractometer	Enraf Nonius CAD 4
Radiation (λ/Å)	Mo-Kα (0.71073)
Monochromator	Oriented graphite (002)
Scan mode	ω–$3\theta/2$
Scan/°	$1+0.35\tan\theta$
Recording range θ/°	2–45
Range of h, k, l	−13 to 13, −10 to 10, 0–23
Intensity decay (%)	1.5
Reflections for crystal matrix orientation ($18°<\theta<24°$)	25
No. of recorded reflections	7302
No. of independent reflections	3726
μ/cm^{-1}	410.1
Absorption correction	Refined on ΔF
T_{min}	0.122
T_{max}	0.777
R_{int} (%)	1.66
No. of independent reflections (N) with $I>3.0\sigma(I)$	2342
Weighting scheme, w	$1/\sigma^2(F_0)$
R^a	0.0268
wR^b	0.0324
No. of refined parameters (M)	58
Extinction coefficient	0.0181(5)

$^a R=\sum\|F_0|-|F_c\|/\sum|F_0|$. $^b wR=[\sum w(|F_0|-|F_c|)^2/\sum w|F_0|^2]^{1/2}$, isotropic secondary extinction (Type I) Gaussian distribution.[36]

Full crystallographic details, excluding structure factors, have been deposited at the Cambridge Crystallographic Data Centre (CCDC). See Information for Authors, 1999, Issue 1. Any request to the CCDC for this material should quote the full literature citation and the reference number 1145/139.

2.3 Absorption corrections

The crystal selected for the structure determination was a thin platelet, which is not a favorable shape for precise absorption corrections. In the past, we have had excellent results using classical methods of absorption correction, such as Gaussian type, based on the precise measurement of the crystal morphology.[17] However, from time to time, the application of this method gave unsatisfactory results. In this context, we decided to test several methods of absorption correction (analytical,[18] Gaussian,[19] semi-empirical based on ψ-scans[20] and a refined method based on ΔF[21]) and to compare them to the uncorrected intensity measurements. The best fit (*i.e.* lowest peak of electronic residues, lowest R_{int} and lowest conventional R factor) was obtained with DELABS, the PLATON98[22] implementation based on the DIFABS[21] algorithm. Then, the final refinements were performed with this correction, after verifications that some cautions had been taken: we ensured

Table 2 Atomic coordinates and displacement parameters

Atom	x	y	z	B^a/Å^2
W1	0.32980(2)	0.25	0.94122(2)	0.401(2)[a]
W2	0.00268(2)	0.25	0.18918(1)	0.367(3)[a]
W3	0.64804(2)	0.25	0.68739(1)	0.357(3)[a]
P	0.6660(1)	0.25	0.40282(9)	0.45(2)[a]
K[b]	0.1399(3)	0.25	0.4975(2)	1.57(5)[a]
O1	0.1703(4)	0.25	0.0707(2)	0.54(3)
O2	0.4981(4)	0.25	0.8078(3)	0.63(4)
O3	0.5	0.5	0.0	0.74(4)
O4	0.1564(3)	0.0004(4)	0.8686(2)	0.81(3)
O5	0.8541(5)	0.25	0.3347(3)	0.92(4)
O6	0.8181(3)	0.0014(5)	0.7291(2)	0.83(3)
O7	0.7475(4)	0.25	0.5272(3)	0.58(3)
O8	0.5454(3)	0.4874(5)	0.3817(2)	1.11(3)

Atom	U_{11}	U_{22}	U_{33}	U_{12}	U_{13}	U_{23}
W1	0.00492(2)	0.00505(4)	0.005279(7)	0.0	0.000261(9)	0.0
W2	0.00444(2)	0.00467(5)	0.004832(9)	0.0	0.00029(1)	0.0
W3	0.00462(2)	0.00443(4)	0.004475(8)	0.0	0.00003(1)	0.0
P	0.0054(1)	0.0078(3)	0.00389(5)	0.0	0.00086(7)	0.0
K[b]	0.0154(4)	0.0158(7)	0.0275(2)	0.0	−0.0111(2)	0.0

[a] $B_{eq} = 8\pi^2 U_{eq}$ with $U_{eq} = \frac{1}{3}\sum_{i=1}^{3}\sum_{j=1}^{3} U^{ij} a_i^* a_j^* \boldsymbol{a}_i \boldsymbol{a}_j$. [b] Statistical occupation = 0.506(3).

that the goniometer was perfectly aligned, that the crystal was sufficiently small to stay entirely in the middle part of the incident X-ray beam; finally, the correction was applied after a refinement performed with B_{iso} and no extinction correction. Note that the different previous methods do not affect significantly the atomic positions and consequently the interatomic distances. On the other hand, they have a noticeable effect on the thermal displacement parameters of the atoms.

2.4 Transport measurements

Resistivity and magnetoresistivity were measured by the four-probe method. Thermopower (TEP) data were obtained by an ac relaxation method. Electrical contacts were made by thermal evaporation of silver pads on a surface cleaned with ammonia. Gold wires (diameter = 25 μm) were attached on the evaporated areas by silver paste. The current was always parallel to the (***a***, ***b***) plane. The calibration of TEP was carried out by using a high purity piece of lead.[23]

3 Results and discussion

3.1 Description of the structure

As usual for members of the MPTBh family, the atomic arrangement of $K_xP_4W_{12}O_{44}$ can be described within the frame of a layer structure built up of regular WO_3-type slabs with the same width ($c\sin\beta = 5.35$ Å), linked together through isolated PO_4 units. Each slab is formed of a set of linear strings of three WO_6 octahedra sharing corners, all oriented with the same direction, approximately [$\bar{1}$01], into a slab and also in the different slabs [Fig. 2(a)]. Fig. 3 and 4 are good illustrations

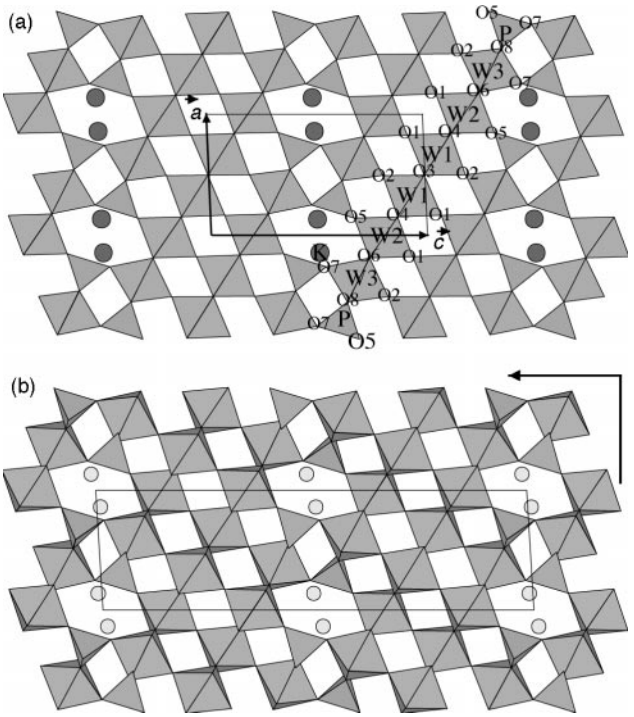

Fig. 2 (a) Projection along b of the $K_xP_4W_{12}O_{44}$ monoclinic structure, (b) $Na_xP_4W_{12}O_{44}$ projection along b showing the tilting of the WO_6 string in a slab and in two adjacent slabs.

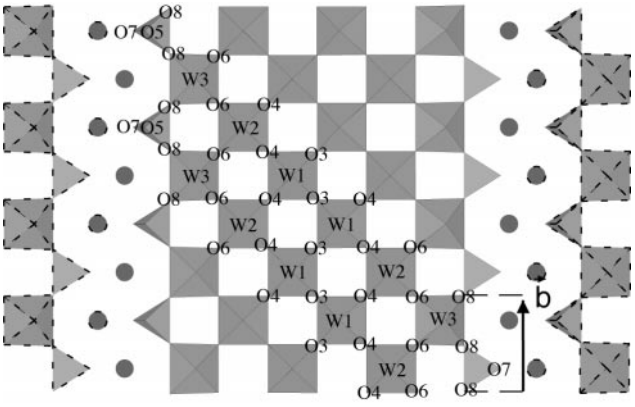

Fig. 3 $K_xP_4W_{12}O_{44}$ section of a slab of WO_3-type normal to an axis of the WO_6 octahedron.

of the WO_3-type slabs regularity in their middle part and of the small distortion on their sides. The O–O distances appear to be essentially identical for the two W(1)O_6 and W(2)O_6 octahedra and range from 2.65 to 2.77 Å with the windows of the different perovskite cages being square shaped. The W(3)O_6 octahedron is slightly distorted and tilted with respect to the other two and is linked to three PO_4 tetrahedra on the side of a slab. Consequently, its O(2)–O(7) axis has an orientation slightly different with respect to the O(2)–O(1)

Table 3 Selected interatomic distances (Å) in $K_2P_4W_{12}O_{44}$

W1–O1	1.912(3)	W2–O1	1.839(3)	W3–O2	1.785(3)
W1–O2	1.986(3)	W2–O4 (×2)	1.825(2)	W3–O6 (×2)	1.804(3)
W1–O3 (×2)	1.870(1)	W2–O5	2.034(4)	W3–O7	2.047(3)
W1–O4 (×2)	1.944(2)	W2–O6 (×2)	2.020(2)	W3–O8 (×2)	2.055(3)
	P–O5	1.525(2)	P–O8 (×2)	1.519(3)	
	P–O7	1.554(4)			
	K–O5	2.656(4)	K–O7 (×2)	2.800(1)	
	K–O6 (×2)	3.038(3)	K–O7	2.659(3)	
	K–O8 (×2)	2.860(3)			

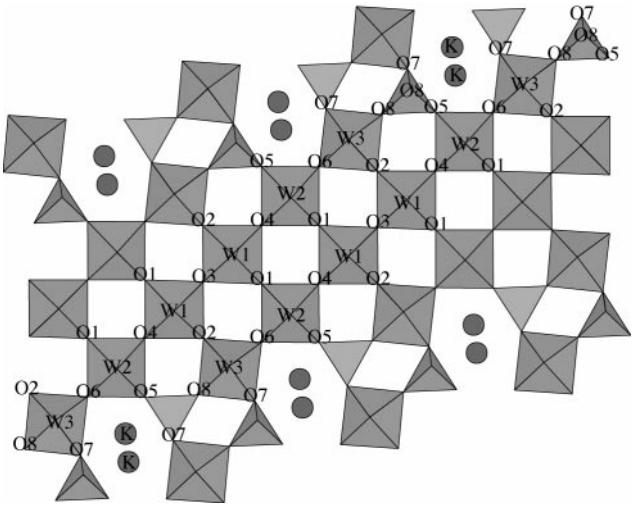

Fig. 4 $K_xP_4W_{12}O_{44}$ oblique section—one octahedron thick—in a WO_3-type slab showing the sequence of six WO_6 octahedra bound to two PO_4 tetrahedra.

and O(1)–O(5) axes of the other two octahedra $W(1)O_6$ and $W(2)O_6$ (Fig. 4). Also the O(8)–O(8) distance in this octahedron (Fig. 3) is the longest [2.811(4) Å]. A similar effect is observed in the PO_4 tetrahedron for which the O(8)–O(8) distance is the longest [2.542(4) Å], the sum of these two O(8)–O(8) distances giving the value of the ***b*** parameter. This is related to the capability of a PO_4 tetrahedron to replace a WO_6 octahedron in a WO_3-type lattice. On the other hand, the edge O(5)–O(7) of the tetrahedron in the (***a***, ***c***) plane is the smallest [2.429(4) Å]. This distortion of the tetrahedron is consistent with a slight elongation of the O–O distance along ***b*** and with a slight shortening in a perpendicular direction.

In this crystal structure, one observes an evolution of the W–O distances in the different WO_6 octahedra which is similar to that observed in the MPTBp $(PO_2)_4(WO_3)_{2m}$ family.[24] Indeed if one compares (Fig. 5) the dispersion of the W–O distances in the different WO_6 octahedra, for a given K compound, one concludes that the dispersion is weak when a WO_6 octahedron is surrounded only by other identical octahedra sharing corners. The dispersion increases when the W atom deviates from the center and is located closer to the PO_4 tetrahedra. If an octahedron is linked to one tetrahedron and thus to five other octahedra, the dispersion of the W–O distances inside a WO_6 octahedron becomes clearly 3+3, and the dispersion is further increased if the surrounding is constructed of three tetrahedra and three octahedra. Indeed, we obtain for both $m=6$ and 7 structures, three W–O distances of *ca.* 1.80 Å and three others of *ca.* 2.05 Å. This difference is slightly reduced for $m=4$ (1.82–2.02 Å) for which the thickness of the slabs is the lowest. Calculations of the tungsten bond valences (v) from the interatomic W–O distances[25] lead to a number of conduction electrons per W-atom, $n=6-v$, which appears to vary with the tungsten atomic position in the WO_3-type slab (Fig. 5) as previously described for the MPTBp compounds $(PO_2)_4(WO_3)_{2m}$.[26] The highest value of the electron density is thus found (whatever the value of m) for the tungsten atoms located in the middle part of the WO_3-slab. This implies that the conduction electrons are mainly confined in the central part of each perovskite slab, in agreement with the 2D character of the compounds.

As already described in detail for the structure of $Pb_{0.66}P_4W_{14}O_{50}$,[12] the 'hexagonal tunnel' of the monophosphate tungsten bronzes MPTBh results from the stacking along ***b*** of large cages, bounded by 18 oxygen atoms, which are joined to each other by means of oblique hexagonal windows. The mean plane of these windows is not perpendicular to ***b*** [Fig. 2(a)], but makes an angle of *ca.* 45° with this direction. Each cage

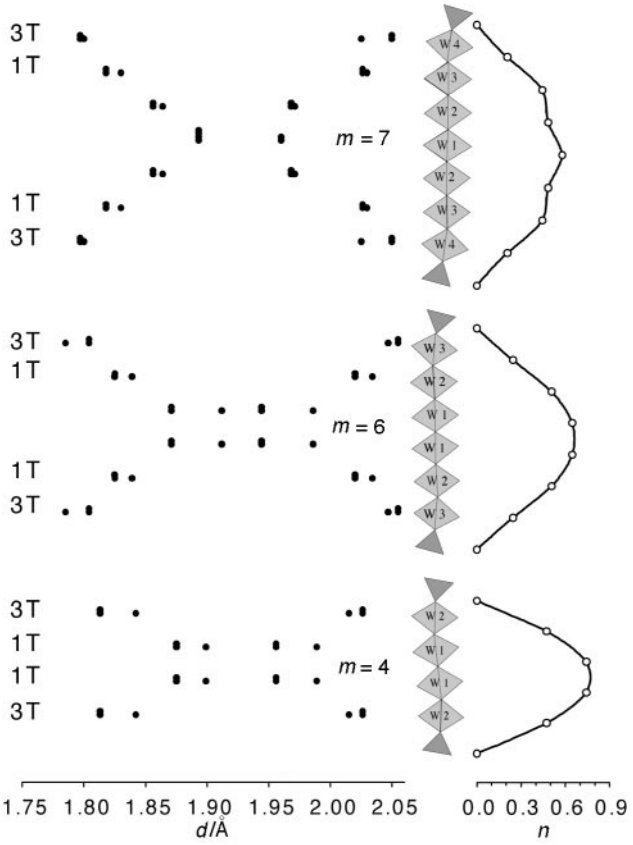

Fig. 5 Dispersion of the W–O distances in the WO_6 octahedra in the $K_x(PO_2)_4(WO_3)_{2m}$ series. 1T and 3T are related to the number (one or three) of PO_4 tetrahedra linked to the WO_6 octahedron. The number of conduction electrons (n) per W atom is highest in the middle of the WO_3-type slab.

contains only one potassium site; the two K positions, visible in Fig. 2(a) and 4, are thus distributed in two adjacent cages. Each site is partially and statistically occupied: no order or particular cationic distribution involving satellites or superstructure reflections have ever been observed with crystals of this family at room temperature. Inside an O_{18} cage, the K site is clearly off-centered, with an anisotropic oxygen surrounding (2+4+2). The two shortest K–O distances (2.66 and 2.68 Å) are established with the oxygens O(5) and O(7) building the edge of a PO_4 tetrahedron and the two longest ones (3.05 Å) are located in the same side of the cage (Fig. 6). The four intermediate distances (2.80 and 2.85 Å) complete coordination to K. It should be noted that nearly the same oxygen surrounding is observed for K in the compounds $K_{0.84}P_4W_8O_{32}$[9] and $K_{1.4}P_4W_{14}O_{50}$,[11] whereas the oxygen environment of the Na atoms is clearly different from one member to another. Thus, four Na–O distances of *ca.* 2.8 Å are observed in $Na_{1.7}P_4W_{14}O_{50}$[10] which are not observed in the Na–oxygen arrangement of $Na_{1.5}P_4W_8O_{32}$ or $Na_{1.7}P_4W_{12}O_{44}$.[8]

3.2 Symmetry in the MPTBh family

The small differences in the interatomic distances previously mentioned are only smooth modifications among similar structures. The lattice parameters of the three known $m=7$ crystal structures (Table 4) with Na, K and Pb as inserted cations are nearly the same.[10–12] Only a slight increase of the cell volume is observed due probably to the cation size. On the other hand, the ***c*** lattice parameter of the $m=4$ and 6 members is twice as large in the Na compounds compared to the K compounds, whereas the lengths of the other parameters are unchanged. Moreover, comparison of the space groups of the different crystals suggests modifications in the atomic frame-

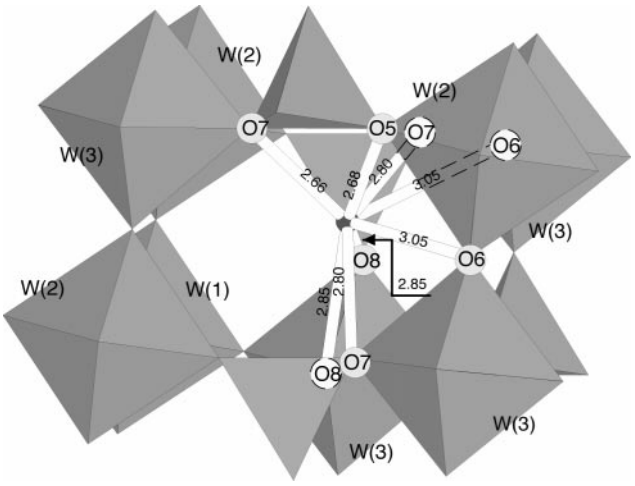

Fig. 6 Location of the K^+ ion into an O_{18} cage. The cage is bounded by eight WO_6 octahedra and four PO_4 tetrahedra. The eight nearest oxygen atoms of a K^+ ion are situated in the same side of the cage involving an anisotropic surrounding of the cation.

work. In this respect, one can compare the title compound $K_xP_4W_{12}O_{44}$ with its Na-based analogue $Na_xP_4W_{12}O_{44}$.

Both have monoclinic symmetry and exhibit a similar single phase domain ($1.2 \leqslant x \leqslant 3$). The major structural difference lies in the fact that the WO_6 octahedra of the Na structure are tilted (*ca.* 8°). Along a given string in a slab of WO_3-type, all the octahedra are tilted with the same orientation, whereas they are tilted with the opposite orientation in the next slab at the same *y* level [Fig. 2(b)]. These orientations are related to each other through a *c* glide plane. By contrast, the WO_6 octahedra in the K structure are not tilted so that two adjacent slabs superimpose through a ***c*** translation. As the $P2_1$ space group is consistent with the observations and cannot *a priori* be ruled out, the existence of an *m* mirror normal to ***b*** has been verified by studying systematically the electronic density about each oxygen site. No anomaly such as splitting or scattering has been detected so that the existence of the *m* mirror plane is established.

3.3 Transport properties

Four single crystals selected from the same batch and corresponding to a K^+ content $x = 2.02(9)$ have been investigated. The resistivity measurements (Fig. 7) reveal two kinds of behavior: for two samples (type A), a linear behavior of the resistivity *vs.* temperature is observed, characteristic of a metal, whereas for the two other crystals (type B), a plot of ρ *vs.* temperature shows a hump.

For all samples, a positive transverse magnetoresistance $\Delta R/R(0)$, when the magnetic field is parallel to the $\boldsymbol{c}^*$ axis, is observed at low temperatures (Fig. 8). For each ρ *vs.* *T* curve, a typical value of magnetoresistance at 7.5 T and 4.2 K is associated: $\Delta R/R(0) \approx 35\%$ for the samples showing a linear ρ *vs.* *T* curve (type A) *cf.* $\Delta R/R(0)$ of $\approx 350\%$ for type B. For type A samples, the angular dependence of $\Delta R/R$ at 7.5 T and 4.2 K shows an ($\boldsymbol{a}\cos\theta$) law, while for type B samples, a large anisotropy is observed which is a deviation from the cosine law expected for a two-dimensional system. For type A, the magnetoresistance increases linearly with field while for type B, two weak anomalies at *ca.* 3.5 and 4.8 T are superimposed on the quasi-linear behavior.

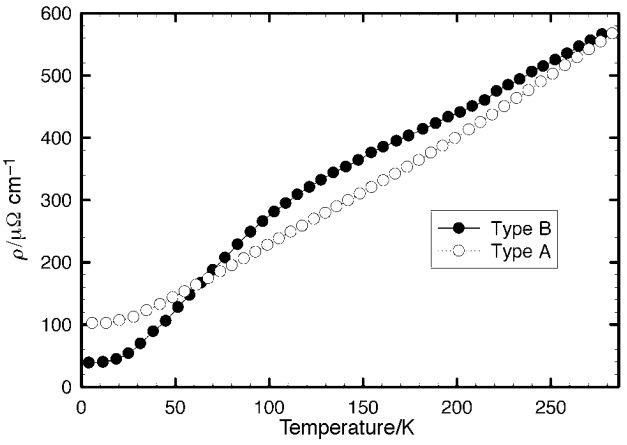

Fig. 7 Resistivity *vs.* temperature for $K_2P_4W_{12}O_{44}$.

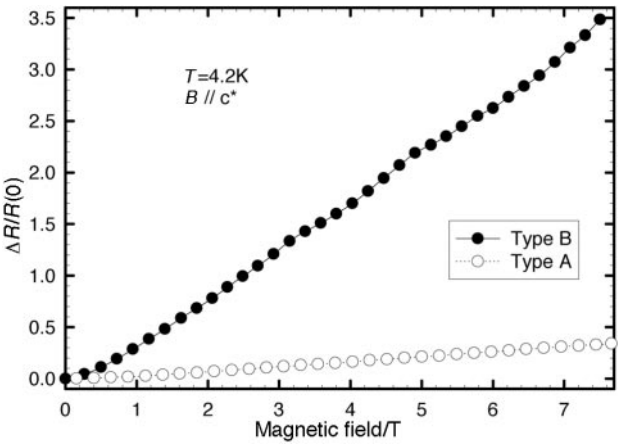

Fig. 8 Magnetoresistance *vs.* magnetic field.

No significant differences in the TEP measurements were found for the two set of crystals: the absolute value of TEP increases monotonously upon increasing temperature as seen in Fig. 9. The sign of TEP gives information on the dominant charge carriers. For these bronzes the dominant charge carriers are electrons over the whole temperature range.

The two behaviors observed in the resistivity may be due to the presence of different amount of defects or impurities. Type B samples may show weak charge density wave (CDW) instabilities. This is consistent with the large magnetoresistance observed in these samples: $\approx 350\%$ at 7.5 T and 4.2 K. It is indeed larger than in $(PO_2)_4(WO_3)_{2m}$[27,28] (for $m = 6$ the MR is of the order of 100% at 7.5 T and 4.2 K) or in $K_xP_4W_8O_{32}$ ($\approx 20\%$).[6,7] Such a behavior is attributed to the presence, on

Table 4 Comparison between the crystallographic data of the seven known compounds in the MPTBh series (for suitable comparison, *a* and *c* parameters have been permutated with respect to literature references for $m = 4$ and 6 Na-based compounds)

	m	Space group	*a*/Å	*b*/Å	*c*/Å	*β*/°	*α*, *γ*/°	*V*/Å^3
$K_{0.84}P_4W_8O_{32}$	4	$P2_1/m$	6.6702(5)	5.3228(8)	8.9091(8)	100.546(7)		310.8
$Na_{1.5}P_4W_8O_{32}$	4	$P2_1/c$	6.6075(5)	5.277(4)	17.788(11)	99.64(5)		611.4
$K_{2.012}P_4W_{12}O_{44}$	6	$P2_1/m$	6.6736(2)	5.3543(3)	11.9005(5)	92.615(3)		424.8
$Na_{1.7}P_4W_{12}O_{44}$	6	$P2_1/c$	6.588(2)	5.291(1)	23.775(17)	93.47(4)		827.2
$K_{1.4}P_4W_{14}O_{50}$	7	$A2/m$	6.660(2)	5.3483(3)	27.06(5)	97.20(2)		956.6
$Na_{1.7}P_4W_{14}O_{50}$	7	$A\bar{1}$	6.575(2)	5.304(1)	27.076(3)	96.17(1)	89.62(1), 90.26(1)	937.1
$Pb_{0.66}P_4W_{14}O_{50}$	7	$A\bar{1}$	6.6015(3)	5.3156(4)	27.039(2)	96.757(5)	90.208(6), 89.867(5)	944.2

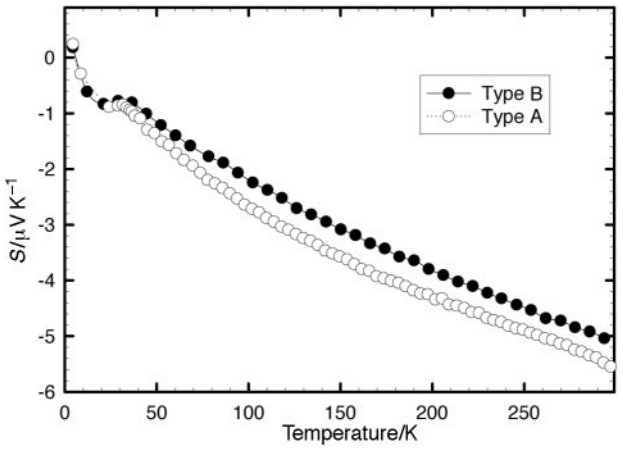

Fig. 9 Thermopower *vs.* temperature.

the Fermi surface, of both electron and hole pockets with high mobilities and is typical of a CDW state. The two small humps seen in Fig. 9 and the anisotropic angular dependence of magnetoresistance could be associated with weak Shubnikov–de Haas oscillations. Low temperature and high magnetic field measurements would be helpful to check this point.

The linear behavior of the thermopower above 100 K is characteristic of a metal. One can evaluate the Fermi energy in a simple one-band model from the slope of S *vs.* T through the formula $S=-\pi^2k_b{}^2T/2|e|\varepsilon_F$.[29] One obtains values of the order of 2.45 eV, larger than found in the undoped bronzes $P_4W_{12}O_{44}$ ($\varepsilon_F \approx 2.3$ eV). It is surprising that both types of samples, A and B, show approximately the same temperature dependence of the thermopower at low temperature. Crystal inhomogeneities may be at the origin of the differences between the two samples as shown from resistivity measurements. According to a previous high resolution electron microscopy study carried out on K-based MPTBh's,[30] different kinds of defects can be taken into account, involving either the distribution of K^+ cations in the O_{18} cages or the distribution of insulating phosphate planes with respect to the conducting WO_3-type slabs.

4 Conclusions

The member $m=6$ of the MPTBh series $K_x(PO_2)_4(WO_3)_{2m}$ has been characterized by single crystal X-ray diffraction and electron transport measurements. As for the previously studied members $m=4$ and 7, the structure can be described as built up from perovskite WO_3-type slabs connected through PO_4 tetrahedra. By contrast to the Na-based analogue $Na_xP_4W_{12}O_{44}$, no tilting of the WO_6 octahedra has been detected. This absence of tilting in $K_xP_4W_{12}O_{44}$, and also in the $m=4$ and 7 members of the series, is a surprising result. Usually, the associations of polyhedra involving WO_3-type structure imply WO_6-octahedra tilting and is observed for all the other monophosphate tungsten bronzes. This is also so for tungsten trioxide WO_3, for the low temperature forms,[31] the room temperature forms, either monoclinic,[32] or triclinic[33] and up to 1170 K for the orthorhombic form.[34] Tilting is also observed in A_xWO_3 bronzes,[35] for example in the different forms of Na_xWO_3, except at the highest concentrations of sodium ($x>0.45$) where Na_xWO_3 becomes cubic. Therefore the tilting of the WO_6 octahedra seems to be a widespread phenomenon, except perhaps for high temperature forms which are not well characterized. As a result we suggest that, from a structural point of view, the room temperature structural forms of the potassium monophosphate tungsten bronzes known at present ($m=4$, 6, 7) might be related to high temperature structures, while the sodium counterparts are related to low temperature structures.

Electrical transport data show quasi-2D metallic behaviour with, for some crystals, huge magnetoresistance effects at low temperature. Such a result suggests the possibility of CDW instabilities. To corroborate this analysis, further physical measurements and structural investigations, especially by X-ray diffuse scattering, are required.

References

1 J. P. Giroult, M. Goreaud, Ph. Labbé and B. Raveau, *Acta Crystallogr., Sect. B*, 1980, **36**, 2570.
2 M. Goreaud, Ph. Labbé and B. Raveau, *J. Solid State Chem.*, 1985, **56**, 41.
3 E. Wang, M. Greenblatt, I. E. I. Rachidi, E. Canadell and M. H. Whangbo, *Inorg. Chem.*, 1989, **28**, 2451.
4 P. Foury-Leylekian, J. P. Pouget, M. Greenblatt and E. Wang, *Eur. Phys. J. B*, 1998, **2**, 157.
5 E. Wang, M. Greenblatt, I. E. I. Rachidi, E. Canadell and M. H. Whangbo, *J. Solid State Chem.*, 1989, **80**, 266.
6 P. Roussel, D. Groult, C. Hess, Ph. Labbé and C. Schlenker, *J. Phys.: Condens. Matter*, 1997, **9**, 7081.
7 S. Drouard, P. Foury, P. Roussel, D. Groult, J. Dumas, J. P. Pouget and C. Schlenker, *Synth. Met., Int. Conf. ICSM'98, Montpellier, France*, 1998, to be published.
8 A. Benmoussa, D. Groult, Ph. Labbé and B. Raveau, *Acta Crystallogr., Sect. C*, 1984, **40**, 573.
9 J. P. Giroult, M. Goreaud, Ph. Labbé and B. Raveau, *J. Solid State Chem.*, 1982, **44**, 407.
10 M. Lamire, Ph. Labbé, M. Goreaud and B. Raveau, *J. Solid State Chem.*, 1987, **66**, 64.
11 B. Domengès, M. Goreaud, Ph. Labbé and B. Raveau, *J. Solid State Chem.*, 1983, **50**, 173.
12 P. Roussel, A. C. Masset, B. Domengès, A. Maignan, D. Groult and Ph. Labbé, *J. Solid State Chem.*, 1998, **139**, 362.
13 *Physics and Chemistry of Low Dimensional Inorganic Conductors*, ed. C. Schlenker, J. Dumas, M. Greenblatt and S. van Smaalen, Plenum, NATO ASI series, 1996.
14 K. Harms and S. Wocadlo, XCAD4, University of Marburg, Germany, 1996.
15 A. Altomare, G. Cascarano, C. Giacovazzo, A. Guagliardi, M. C. Burla, G. Polidori and M. Camalli, *J. Appl. Crystallogr.*, 1994, **27**, 435.
16 V. Petricek and M. Dusek, JANA98, Institute of Physics, Prague, Czech Republic, 1997.
17 P. Roussel, G. Mather, B. Domengès, D. Groult and Ph. Labbé, *Acta Crystallogr., Sect. B*, 1998, **54**, 365.
18 J. de Meulenaer and H. Tompa, *Acta Crystallogr., Sect. A*, 1965, **19**, 1014.
19 W. R. Busing and H. A. Levy, *Acta Crystallogr., Sect. A*, 1957, **10**, 180.
20 A. C. T. North, D. C. Phillips and F. Scott Mathews, *Acta Crystallogr., Sect. A*, 1968, **24**, 351.
21 N. Walker and D. Stuart, *Acta Crystallogr., Sect. A*, 1983, **39**, 158.
22 A. L. Spek, *Acta Crystallogr., Sect. A*, 1990, **46**, C34.
23 R. B. Roberts, *Philos. Mag.*, 1977, **36**, 91.
24 P. Roussel, Ph. Labbé, D. Groult, B. Domengès, H. Leligny and D. Grebille, *J. Solid State Chem.*, 1996, **122**, 281.
25 B. Domengès, N. K. McGuire and M. O'Keefe, *J. Solid State Chem.*, 1985, **82**, 94.
26 C. Hess, C. Le Touze, C. Schlenker, J. Dumas, D. Groult and J. Marcus, *Synth. Met.*, 1997, **86**, 2419.
27 A. Rötger, C. Schlenker, J. Dumas, E. Wang, Z. S. Teweldemedhin and M. Greenblat, *Synth. Met.*, 1997, **55–57**, 2670.
28 C. Hess, C. Schlenker, J. Dumas, M. Greenblatt and Z. S. Teweldemedhin, *Phys. Rev. B*, 1996, **54**, 4581.
29 R. D. Barnard, in *Thermoelectricity in Metals and Alloys*, Taylor & Francis Ltd, London, 1972.
30 B. Domengès, M. Hervieu, B. Raveau and M. O'Keeffe, *J. Solid State Chem.*, 1988, **72**, 155.
31 P. M. Woodward, A. W. Sleight and T. Vogt, *J. Solid State Chem.*, 1997, **131**, 9.
32 B. O. Loopstra and H. M. Rietveld, *Acta Crystallogr., Sect. B*, 1969, **25**, 1420.
33 R. Diehl, G. Brandt and E. Salje, *Acta Crystallogr., Sect. B*, 1978, **34**, 1105.
34 E. Salje, *Acta Crystallogr., Sect. B*, 1977, **33**, 574.
35 Ph. Labbé, in *Diffusionless phase transitions and related structures in oxides*, ed C. Boulesteix, Trans Tech Publications, Zürich, Switzerland, 1992, pp. 293–339.
36 P. J. Becker and P. Coppens, *Acta Crystallogr., Sect. A*, 1974, **30**, 129.

Paper 8/08902G